ARMY RESEARCH LABORATORY

A Novel Soft Recovery System for the 155-mm Projectile and Its Numerical Simulation

by Avi Birk and Douglas E. Kooker

ARL-TR-2462 April 2001

Army Research Laboratory
Aberdeen Proving Ground, MD 21005-5066

ARL-TR-2462 **April 2001**

A Novel Soft Recovery System for the 155-mm Projectile and Its Numerical Simulation

Avi Birk and Douglas E. Kooker
Weapons and Materials Research Directorate, ARL

Abstract

There is a requirement to soft catch, without exceeding a deceleration rate of 1,600 g, and within less than 300 m, an unmodified 102-lb SADARM (Sense and Destroy Armor) projectile fired at 840 m/s. This report presents a soft-recovery concept and its numerical simulation. The concept entails aerodynamic deceleration of the projectile in a long tube attached to the gun barrel. The midsection of the tube is bound between a diaphragm and a free piston and is prepressurized to about 2 MPa. As the projectile enters the tube, the shock wave preceding it ruptures the diaphragm and the projectile decelerates as high pressure builds between it and the free piston. The piston disengages and travels forward scooping water. The waterlog that forms in front of the piston effectively increases the piston's mass and also induces braking force because of the water friction with the tube wall. The projectile's deceleration is controlled, and eventually the projectile exits the tube with a velocity of 10 m/s. The numerical simulation, based on the method of characteristics, incorporates unsteady one-dimensional fluid dynamics that captures the extensive wave dynamics. This report details the effects on the projectile's deceleration of the midsection length, initial pressure, and the water mass. From the simulation, it is possible to soft capture the SADARM projectile within 120 m.

Contents

List of Figures

INTENTIONALLY LEFT BLANK.

List of Tables

INTENTIONALLY LEFT BLANK.

1. Introduction

1.1 The Requirement for a Soft Recovery System

With advances in microelectronic and electro/optic sensors, smart projectiles have become a reality. Such a projectile is the U.S. Army's XM898 SADARM (Sense and Destroy Armor) 155 mm. Because of the sensitive components and packaging inherent to these designs, projectile tests to evaluate performance and/or failure analysis are very expensive. Owing to the projectile's complexity and thin-wall construction, a dummy or malfunctioned projectile recovered after being fired downrange may be too damaged for useful analysis. Hence arose the need for a soft recovery system (SRS) for the XM898 and similar projectiles. Soft recovery is defined here as the recovery of the projectile in a manner that the projectile does not exceed certain deceleration limits and damage thresholds. The foremost proponents of the SRS have been Ami Frydman [1] and Donald Carlucci [2]. The major specifications for the SRS are (1) the projectile is to be fired from a standard gun barrel with standard propellant charge, (2) the projectile shall not be modified in any way, (3) the SRS shall be able to softly catch a projectile fired at 840 m/s within 200 m from the muzzle without exceeding a deceleration level of 1,600 g, and (4) the SRS shall have a rapid-turnaround. The utilization of the SRS will enable the verification of launch integrity and functionality of the projectile's components, by measuring the functional and/or structural performance of the components during the first 1,200 cal. of the projectile's travel. The principal author of this report has proposed a novel SRS concept that fulfills the SRS specifications and is believed to have important advantages when compared to other concepts. This report details a numerical model and its predictions for the flow dynamics in the proposed SRS—work funded by the SADARM Program Management Office to verify the feasibility of the concept and provide a tool for its engineering.

1.2 Soft Recovery Concepts and Systems

Basically, all of the techniques for the soft recovery of fired projectiles had been established over 20 years ago. Some of the techniques were actually tried out; others existed only in the form of patents. However, only a few of the techniques comply with the present specifications for the SRS. Wright [3] gave a comprehensive list of techniques that existed up to the early 1970s. Paul Baer [4] of the U.S. Army Ballistic Research Laboratory (BRL),* Aberdeen Proving Ground, MD proposed an SRS for the 155-mm cannon. He suggested firing the

* The U.S. Army Ballistic Research Laboratory (BRL) was deactivated 30 September 1992 and subsequently became part of the U.S. Army Research Laboratory (ARL) on 1 October 1992.

projectile in a side-vented gun such that the projectile exits with a low velocity into a recovery tube filled with compressed air. The rifled gun tube was to be connected to the recovery tube via a "rotating band squeezer" followed by a diaphragm that would retain the compressed air. Paul Baer simulated numerically the flow in his proposed SRS, but used a lumped parameter approach that completely ignored the very important wave motion that can produce large peaks of projectile deceleration. A major drawback of Baer's SRS is the requirement to modify the gun by the side vent. In the early 1980s, Honeywell Inc. [5] constructed an SRS for BRL and the system was tested successfully with a 155-mm cannon [6]. Although the Honeywell system had the advantage of being able to accommodate multiple calibers, it had a major drawback—it required a modification of the projectile. The system employed a water scoop mounted to the projectile that slowed the projectile via momentum exchange with water in a trough. The projectile also was modified during flight because the technique required the stripping of the projectile's A (rotating) band. A physically sound concept for an SRS is the Ballistic Compression Decelerator patented by the McDonnell Douglas Corporation in 1972 [7]. The projectile is fired into a prepressurized succession of "decelerator tubes" that are separated by multiple diaphragms such that the pressure builds up ahead of the projectile (thus decelerating it), and the diaphragms rupture before being pierced by the projectile.

An SRS based on the McDonnell Douglas patent is presently in operation [1, 2] at the German firm Rheinmetall W&M, and this SRS is the main competitor for the SRS proposed in this report. It can stop an 840 m/s 155-mm projectile in 200 m. The main disadvantage of the multiple decelerator tube concept is that it employs long tubes, and multiple diaphragms. Therefore, it is expensive to construct and it occupies a large amount of real estate. A variation on the ballistic compression concept is the McDonnell Douglas 1976 patent [8] titled "Projectile Recovery System With Quick Opening Valves." Here, quick opening valves that unseal the tube as the projectile approaches them replace the diaphragms. This concept is considered impractical because of its reliability. Two patents that do not rely on ballistic compression are the "Rifled Soft Recovery System," [9] and "Multicaliber Projectile Soft Recovery System" [10]. The rifled concept relies on a spinning projectile being accurately reengaged in a recoiled rifled tube. This concept requires great precision of the firing cycle and tube alignment; it is not proven and will probably subject the projectile to balloting and excessive stresses. The multicaliber concept has the advantage (unlike ballistic compression) of handling multi calibers for the same SRS. A deformable element is placed in the path of the projectile and the projectile becomes embedded in the element. Mechanical forces are applied to stop the element. This concept lacks the deceleration control that the ballistic compression technique has, and it subjects the projectile to excessive forces upon embedding.

2. The Proposed Soft Recovery System

The proposed SRS concept for the 155-mm projectile is based on the ballistic compression principle. It is sketched in Figure 1. Unique to the concept is the incorporation of a water-controlled free piston in the decelerator tube. The principle of operation is as follows. The atmospheric transition tube (ATT) has rifling that continues the barrel's rifling. The rifling is tapered and it transitions to a smooth barrel. The spin-stabilized 155-mm projectile enters the ATT where the tapered rifling in the tube gradually compresses the projectile's rotating band such that the band engraving is squeezed out and a good seal is formed between the band and the smooth wall portion of the ATT. The tapered rifling is believed to alleviate balloting of the projectile in the tube. The band sealing assures that compressed gas in front of the projectile will not leak around the projectile. The combustion gases behind the projectile escape through the vent holes in the ATT and the pressure on the projectile's rear face effectively drops to atmospheric value. The shock wave that precedes the projectile ruptures the 750-psi diaphragm that holds the pressurized air and enters into the pressurized tube. When the shock wave reaches the free piston and reflects from it, the free piston overcomes the shear ring that holds it against the pressurized air. The free piston then moves down the guide tube pushing ahead a growing column of water. The free piston is made of light material, e.g., plastic such as high-density polyethylene. The free piston has to be light enough so that initially it accelerates quickly and thus prevents high-pressure spikes from developing in the pressurized tube section. The water effectively increases the free piston mass with time and also adds frictional force due to the water boundary layer on the tube wall. The growth of the free piston mass and the added water friction retard the free piston motion and thus regulate the air pressure between the free piston and the projectile to a sustained level between 2,000 and 4,000 psi. This pressure is enough to slow the projectile from 840 m/s to 10 m/s within 100 m without exceeding the 1600-g deceleration limit. The water and compressed air escape in the slotted brake tube, and the projectile is stopped in the tapered lining of the brake tube. In operation of the SRS, the initial pressure and water mass are easily adjusted to allow fine control of the projectile exit velocity into the brake tube.

The expendable parts in this SRS concept are the diaphragm, the shear ring, and the free piston. Because the proposed SRS length is much shorter than the aforementioned Rheinmetall's SRS and it employs fewer expendable parts, it is believed that the construction and operation of the proposed SRS is significantly cheaper than Rheinmetall's SRS.

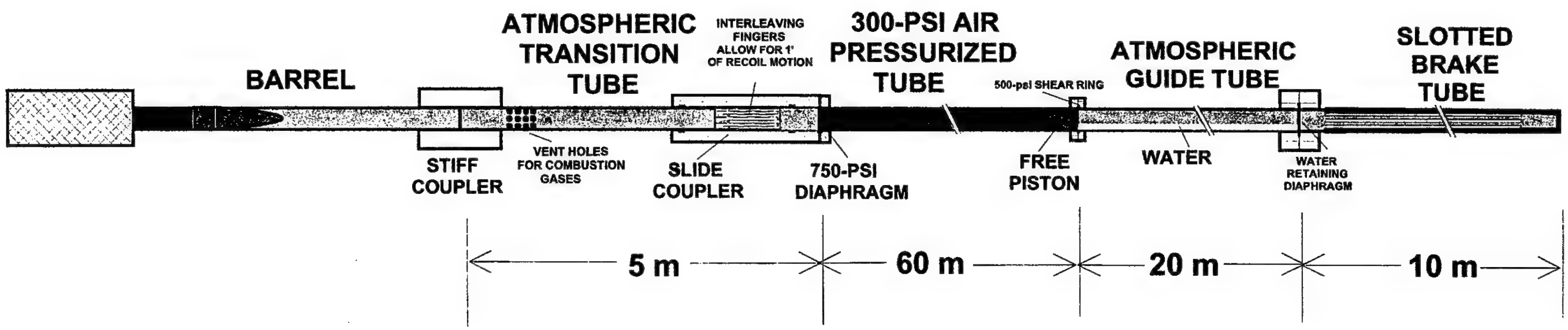

Figure 1. The proposed soft recovery system concept.

3. Mathematical Model of the Flow Dynamics in the SRS Tube Sections

A numerical model was constructed to simulate the transient flow fields generated in the SRS tube. The model consists of four separate zones linked by boundary conditions across the projectile, the free piston, the two shock waves, and the exit plane (Figure 2).

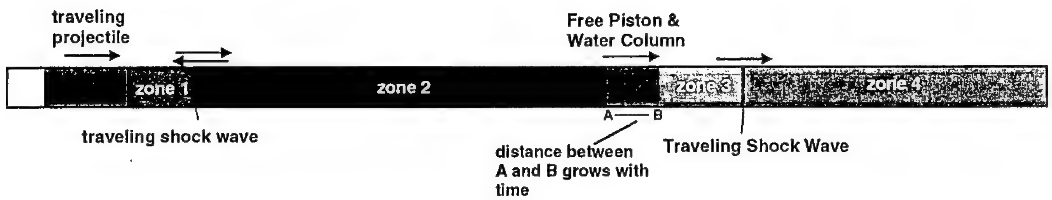

Figure 2. The zonal construction of the SRS tube flow.

Zone 1 is between the projectile and the traveling shock wave that originally is generated by the supersonic entry of the projectile into the tube. Zone 2 is the region between this traveling wave and the free piston. Initially, the shock wave leading the projectile reflects from the rupture diaphragm (the diaphragm is located in zone 2, although it is not shown in Figure 2). The diaphragm should rupture upon reflection, thus initiating the transient flow in the pressurized gas between the diaphragm and the free piston. When the pressure on the free piston exceeds a certain value, the free piston overcomes the shear ring that holds it against the pressurized air and begins its motion. The traveling wave may reflect a few times between the free piston and the projectile until the free piston has exited the tube. In the numerical solution procedure, the decision to reflect the wave from either the projectile or the free piston is made when the thickness of zones 1 or 2 becomes less than 1% of the distance between the projectile and free piston.

Zone 3 is between the front of the water column and the traveling shock wave generated by the fast acceleration of the free piston. The water column thickens as the free piston sweeps the water layer ahead of it. The water column forms in front of the piston because the piston velocity is 1 order of magnitude greater than the water gravity wave (for wave amplitude that equals the tube diameter). Zone 4 is between the traveling wave and the tube's exit. Zone 4 disappears when the traveling wave reaches the exit, and at this time zone 3 becomes the region between the free piston and the exit. Then, zone 3 disappears when the front of the water column reaches the exit plane and the free piston exits the tube. Zone 2 disappears when the traveling wave between zones 2 and 1 reaches the exit, and at this time zone 1 becomes the region between the projectile and the exit.

The time-dependent governing equations in each zone assume isentropic flow of a Noble-Abel gas with constant molecular weight, covolume, and ratio of specific heats. Furthermore, the flow is assumed to be one-dimensional and inviscid, which of course neglects heat transfer to the tube wall. The one-dimensional treatment of the problem necessarily assigns a flat front to the projectile, a front that in reality is an elongated ogive. Obviously, boundary layer effects are not accounted for. In practice, the growth of boundary layers in the long sections of the tube will constrict the flow and modify the strength of the traveling shock waves. Intuitively, viscosity and boundary layer effects will tend to dissipate the wave motion in the tube thus resulting in lower peak pressure loading (and hence deceleration) on the projectile. Thus, the simplified assumptions are likely to result in conservative peak pressure values. The present model incorporates the most important aspects of the flow physics and it is therefore adequate for the purpose of feasibility studies of the SRS concept, and for a parametric study of the concept.

With pressure P, density ρ, velocity u (with respect to laboratory coordinates), and sound speed a, these equations can be written in characteristic form as

$$\frac{dP}{dt} \pm \rho \cdot a \cdot \frac{du}{dt} = 0, \tag{1}$$

which are integrated, respectively, along the right (+) and left (–) running directions,

$$\frac{dz}{dt} = U \pm a, \tag{2}$$

where U is the material velocity relative to the coordinate velocity V_c, i.e., $U = u - V_c$. The energy equation can be written in the form

$$\frac{dP}{dt} - a^2 \cdot \frac{d\rho}{dt} = 0, \tag{3}$$

which is integrated along the streamline

$$\frac{dz}{dt} = U. \tag{4}$$

With the temperature T, covolume b, ratio of specific heats γ ($=c_p/c_v$), and gas constant $\Re$ ($\equiv$ universal gas constant/molecular weight), the Noble-Abel equation of state is simply

$$\frac{P}{\rho} = \frac{\Re \cdot T}{1 - \rho \cdot b}, \tag{5}$$

which dictates the sound speed a,

$$a^2 = \left.\frac{dP}{d\rho}\right|_{entropy} = \frac{\gamma \cdot P/\rho}{1-\rho \cdot b}. \tag{6}$$

There are three independent variables here: u, P, and ρ. Two equations are provided by the compatibility conditions in equation 1 along the right and left characteristic directions given by equation 2. The third is the energy equation given in equation 3 which can be solved along the streamline in equation 4. The temperature T follows directly from equation 5.

As previously mentioned, when the coordinate system is in motion, the characteristic directions must be calculated with the velocity relative to the moving coordinate, i.e., $U = u - V_c$. For all calculations discussed here, the end points of each coordinate zone remain attached to the adjacent moving boundary, and the local grid points within the zone are distributed uniformly between the instantaneous boundary locations (like an "accordion"). Hence, the local coordinate velocity varies linearly between the two boundary velocities. This is illustrated schematically in Figure 3 for zone 1 which is attached to the projectile front face and the traveling shock wave.

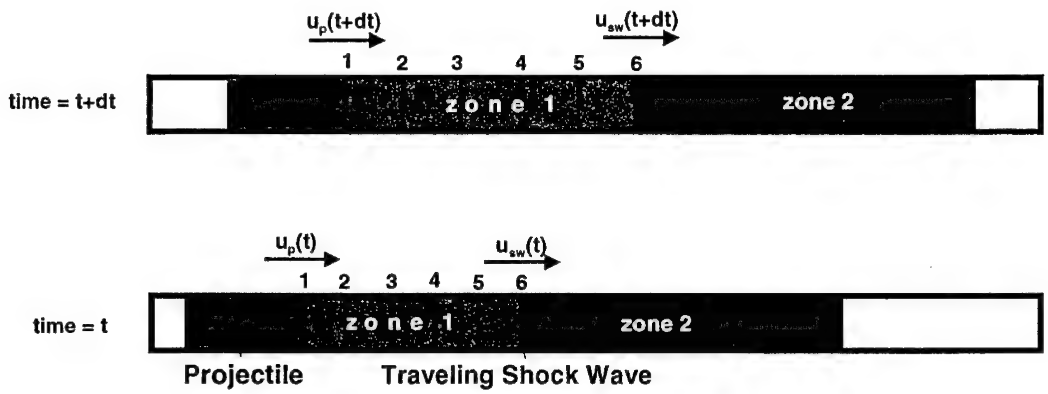

Figure 3. Illustration of numerical coordinate motion with time.

The numerical solution of equations 1 and 3 is determined with the method-of-characteristics (MOC) which to a great extent will faithfully reproduce local wave motion without spurious numerical oscillations. The MOC routines employed here were taken from Kooker [11] where all interpolation is done with Akima splines [12]. All boundary values are also obtained with special routines based on MOC. Motion of the projectile and the free piston within the tube is assumed to be frictionless.

3.1 Solution Methodology

In general, the flow is solved sequentially from zones 1 to 4. For each zone, the boundary conditions must be solved first before the interior flow solution. The solution is known at time t=0 and it is marched from time t to time t+dt using the characteristic/free-stream construct shown in Figures 4-8. All notations are noted in these figures.

3.1.1 The Projectile Boundary Conditions (Figure 4)

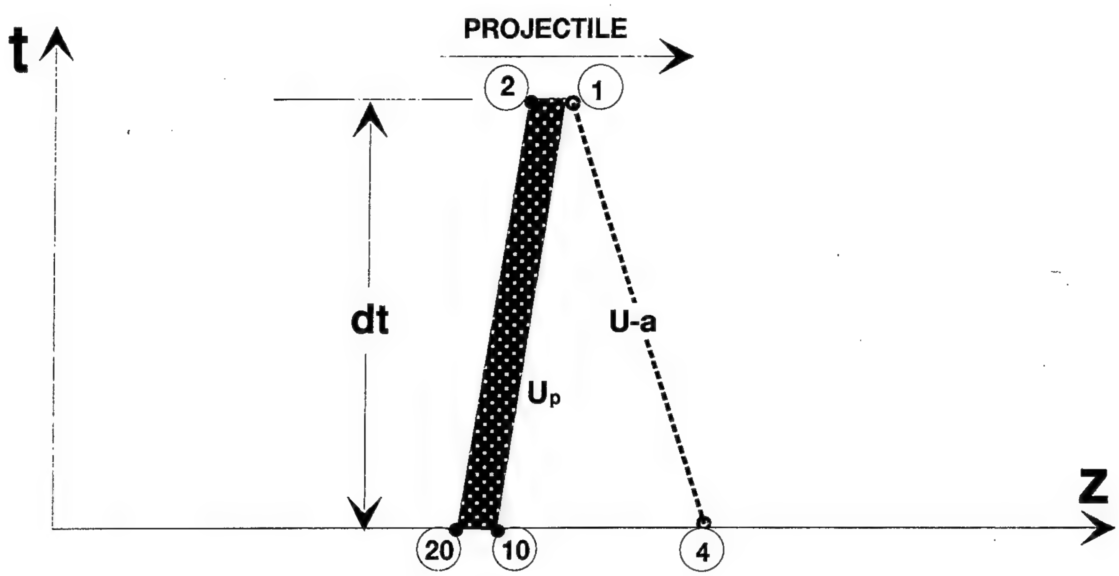

Figure 4. Construct of the projectile's boundary.

From equations 1 and 2, upstream along the 4-1 left-running characteristic:

$$P_1 - P_4 - (\rho \cdot a)_{41} \cdot (u_1 - u_4) = 0, \tag{7}$$

where

$$(\rho \cdot a)_{41} = \left\{ \frac{(\rho \cdot a)_4 + (\rho \cdot a)_1}{2} \right\}.$$

From Newton's Second Law:

$$\sum F = \frac{d(M \cdot V)}{dt},$$

$$\left\{ \frac{P_{20} + P_2}{2} - \frac{P_{10} + P_1}{2} \right\} \cdot A_p = M_p \cdot \left(\frac{u_1 - u_{10}}{dt} \right). \tag{8}$$

M_p and $A_p = \dfrac{\pi \cdot D^2}{4}$ are the projectile mass and cross-section area.

From equations 3 and 4, along the streamline 10-1:

$$P_1 - P_{10} - a_{110}^2 \cdot (\rho_1 - \rho_{10}) = 0, \tag{9}$$

where $a_{110}^2 = \left\{ \dfrac{a_1^2 + a_{10}^2}{2} \right\}$ and a is given by equation 6.

The pressures behind the projectile P_{20} and P_2 are given (assumed to be atmospheric). The values at point 10 are known from the previous step, and the values at point 4 are found using Akima splines interpolation for this point. Thus, the unknowns in equations 7–10 are u_1, P_1, and ρ_1, and they are found by guessing an initial P_1 value and solving equations 7–9 iteratively.

3.1.2 The Free-Piston Boundary Conditions (Figure 5)

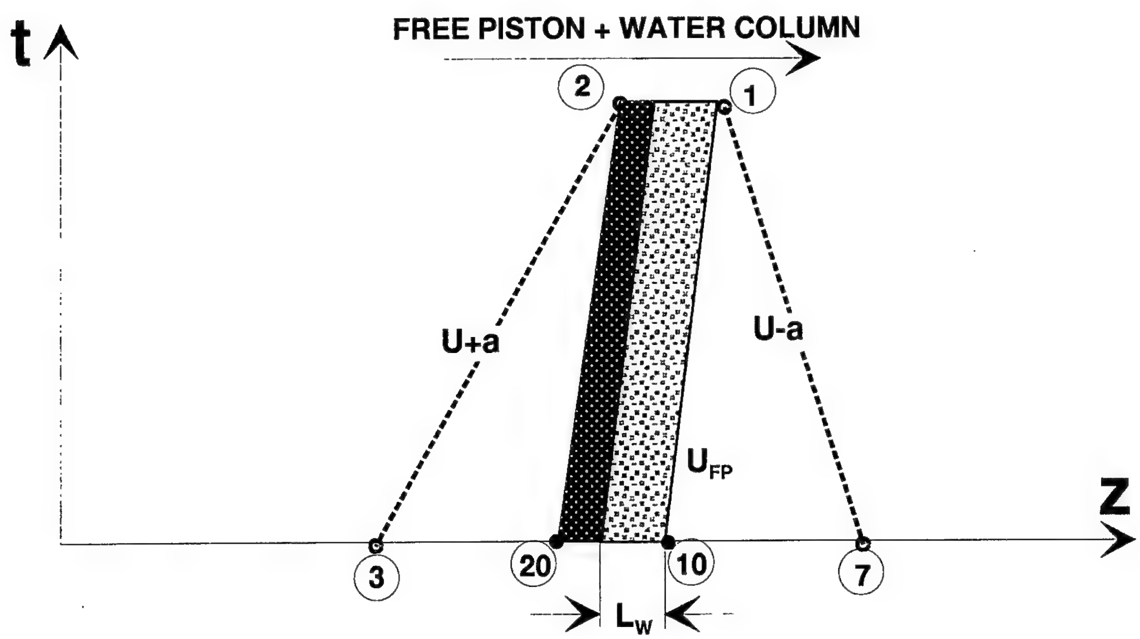

Figure 5. Construct of the free-piston boundaries.

The solution methodology is similar to that of the projectile, with the exception that the right running characteristic has to be solved, and the water column mass and friction have to be accounted for in the force balance equation.

From equations 1 and 2, downstream along the 2-3 right-running characteristic:

$$P_2 - P_3 + (\rho \cdot a)_{32} \cdot (u_2 - u_3) = 0, \tag{10}$$

where

$$(\rho \cdot a)_{32} = \left\{ \frac{(\rho \cdot a)_3 + (\rho \cdot a)_2}{2} \right\}.$$

From equations 3 and 4, along the streamline 20-2:

$$P_2 - P_{20} - a^2_{220} \cdot (\rho_2 - \rho_{20}) = 0, \tag{11}$$

where

$$a^2_{220} = \left\{ \frac{a^2_2 + a^2_{20}}{2} \right\}.$$

Similarly, along the streamline 10-1:

$$P_1 - P_{10} - a^2_{110} \cdot (\rho_1 - \rho_{10}) = 0, \tag{12}$$

where

$$a^2_{110} = \left\{ \frac{a^2_1 + a^2_{10}}{2} \right\}.$$

Upstream along the 7-1 left-running characteristics:

$$P_1 - P_7 - (\rho \cdot a)_{71} \cdot (u_1 - u_7) = 0, \tag{13}$$

where

$$(\rho \cdot a)_{71} = \left\{ \frac{(\rho \cdot a)_7 + (\rho \cdot a)_1}{2} \right\}.$$

From Newton's Second Law:

$$\left\{ \frac{P_{20} + P_2}{2} - \frac{P_{10} + P_1}{2} - \frac{2}{D} \cdot \rho_W \cdot \left(L_W \cdot u^2 \cdot f \right)_{110} \right\} \cdot A_{FP} = \frac{1}{dt} \{ (M_{FP} + M_{W1}) \cdot u_1 - (M_{FP} + M_{W10}) \cdot u_{10} \}, \tag{14}$$

where M_{W10} and M_{W1} are the masses of the water column at time t and t+dt, L_W is the water column length, and M_{FP} and $A_{FP} = A_P$ are the free piston mass and cross- section area.

The frictional force due to the water column,

$$\rho_W \cdot \left(L_W \cdot u^2 \cdot f\right)_{220} \cdot \frac{2}{D} A_{FP} = \rho_W \cdot \left(L_{W2} \cdot u_2^2 \cdot f_2 - L_{W20} \cdot u_{20}^2 \cdot f_{20}\right) \cdot \frac{2}{D} A_{FP},$$

where the friction coefficient is taken from [13] for turbulent flow in a tube (the Prandtl universal law for smooth circular tube).

$$f = \frac{1}{16 \cdot \left(\log_{10}\left(\mathrm{Re}\sqrt{f}\right) - 0.4\right)^2} \quad \text{where } \mathrm{Re} = \frac{\rho_W \cdot u \cdot D}{\mu_W} \text{ is the Reynolds number.}$$

There are six unknowns in equations 10–14, namely: u_1, P_1, ρ_1, and u_2, P_2, ρ_2, where, of course, sound speeds a_1 and a_2 are found from equation 6. The remaining equation relates u_1 to u_2, i.e., $u_1 = (1 + K) \cdot u_2$, where the factor K is the initial ratio of water to air volumes in the guide tube. This solution requires iteration similar to the projectile solution.

3.1.3 Solution for a Grid Point in the Inner Flow (Figure 6)

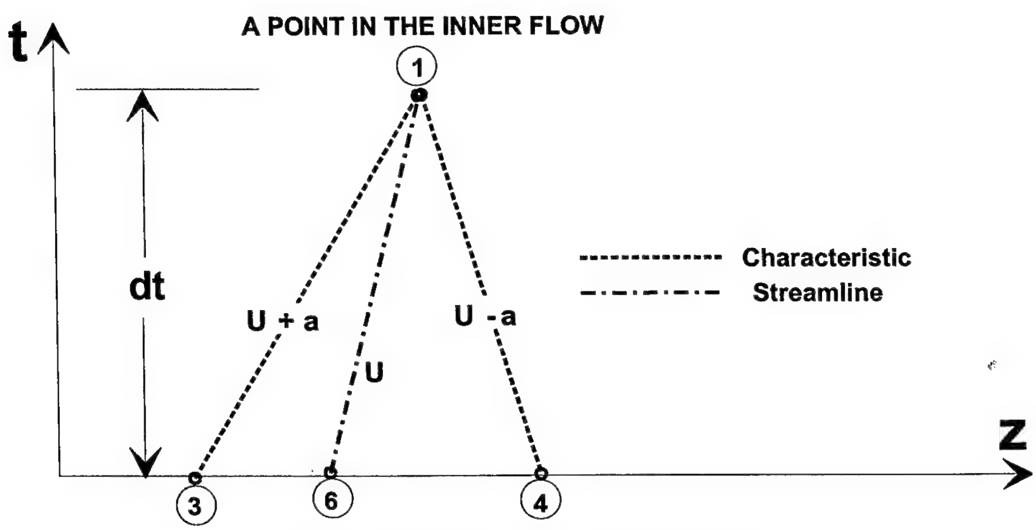

Figure 6. Construct of an inner flow point.

The inner flow solution is based on two characteristics lines (right-running and left-running) and one streamline. The unknowns are u_1, ρ_1, and P_1 which are found from equations similar to equations 10, 11, and 13 (where, again, the sound speed is found from equation 6).

3.1.4 The Shock Wave Boundary Jump Conditions (Figure 7)

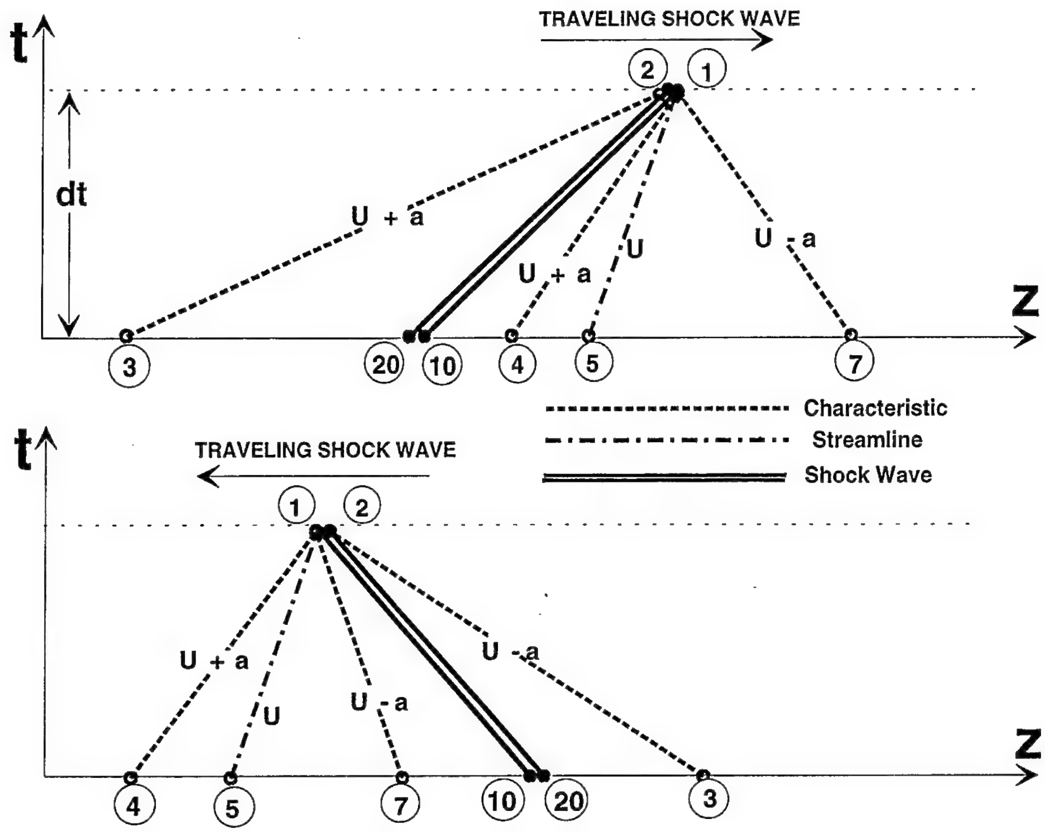

Figure 7. Construct of the traveling shock waves.

Because of the projectile's supersonic velocity, a shock wave leads the projectile's motion. Once the projectile enters the catch tube (that has the same diameter as the projectile), the shock wave detaches from the projectile and becomes a traveling wave. A traveling shock wave will also originate in front of the free piston as the piston accelerates to supersonic velocity.

The values at point 1 (Figure 7) are uniquely determined by the upstream flow field and are found identically to the inner-point solution. The remaining unknowns are u_2, ρ_2, P_2, and u_{SW} (the shock wave velocity), requiring four equations for a solution. The characteristic line trailing the shock wave on the high-pressure side provides one equation. The remaining three equations are jump conditions across the discontinuity to conserve mass, momentum, and energy.

Mass:

$$\rho_2 \cdot (u_2 - u_{SW}) = \rho_1 \cdot (u_1 - u_{SW}); \tag{15}$$

Momentum:

$$P_2 + \rho_2 u_2 \cdot (u_2 - u_{SW}) = P_1 + \rho_1 u_1 \cdot (u_1 - u_{SW}); \tag{16}$$

Energy:

$$e_2 + \frac{P_2}{\rho_2} + \frac{1}{2} \cdot (u_2 - u_{SW})^2 = e_1 + \frac{P_1}{\rho_1} + \frac{1}{2} \cdot (u_2 - u_{SW})^2; \tag{17}$$

where $e = c_V \cdot (T - T_0)$ and T is related to P and ρ through the equation of state (equation 5).

Equations 15–17 can be rearranged such that together with the characteristic equation, they result in two nonlinear algebraic equations that include only u_{SW} and P_2 as unknowns. The numerical solution is obtained by iteration.

3.1.5 The Tube Exit Boundary (Figure 8)

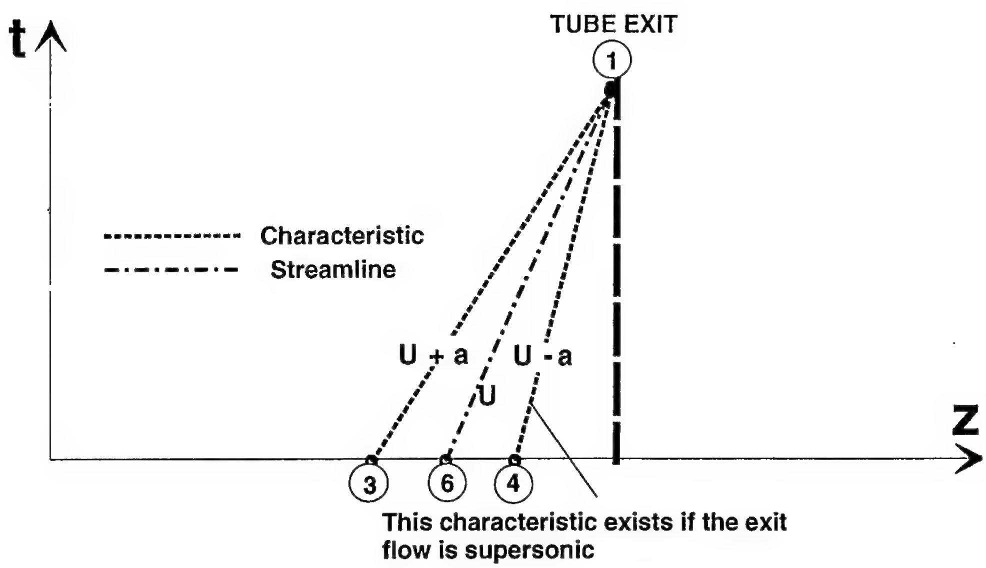

Figure 8. The tube exit boundary.

If the exit flow is supersonic or sonic, the unknowns are u_1, ρ_1, P_1, the solution is like an inner-point solution. If the flow is subsonic, P_1 is atmospheric, and u_1 and ρ_1 are found from the solution of the right-running 3-1 characteristic and the streamline.

The solution methodology is as follows. An initial value of ρ_l is guessed, the equations are solved, ρ_l is updated, and the point 4 is found. If the point lies left of the exit plane, the flow is supersonic, and the equations are re-solved using the two characteristics 3-1 and 4-1 until ρ_l converges. If the point 4 lies right of the exit plane, the flow is subsonic, and the equations are re-solved using only the 3-1 characteristic and the assumption that the static pressure at the exit plane is atmospheric.

3.1.6 The Shock Wave Reflection (Figure 9)

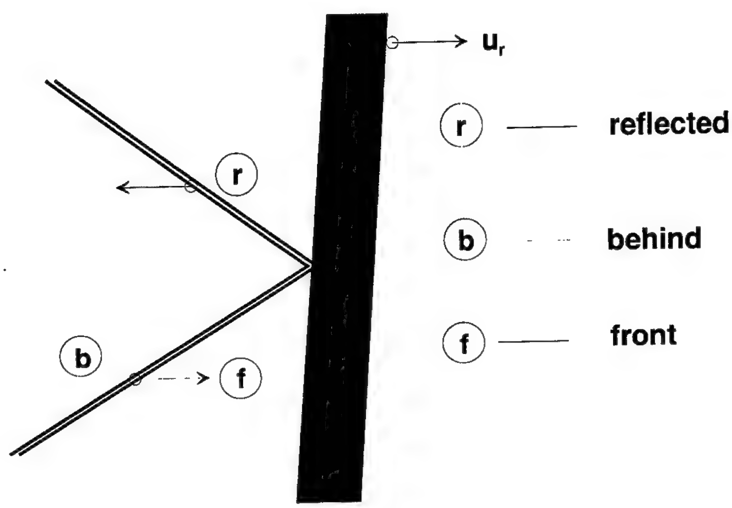

Figure 9. Flow regions in a reflecting shock wave.

The shock wave that separates zone 1 from zone 2 will reflect from the rupture disc, thereby causing a pressure differential across the disc that is sufficient for its rupture. During the flow process, the wave also reflects from both the projectile's face and the free piston's rear.

Figure 9 shows schematically the shock wave reflection process from a boundary that may have a velocity u_r. The flow conditions in the "front" and "behind" regions are known from the preceding shock wave boundary solution. The boundary velocity, u_r, which is also the gas velocity in the reflected region at the boundary, is known from the projectile or free piston boundary solutions. Thus, the unknowns are ρ_r, P_r, and u_{SWr} (the reflected shock wave velocity). These unknowns are easily solved using the conservation of mass, momentum, and energy as in equations 15–17.

Mass:

$$\rho_b \cdot (u_b - u_{SWr}) = \rho_r \cdot (u_r - u_{SWr}); \tag{18}$$

Momentum:

$$P_r + \rho_r \cdot u_r \cdot (u_r - u_{SWr}) = P_b + \rho_b \cdot u_b \cdot (u_b - u_{SWr}); \tag{19}$$

Energy:

$$e_r + \frac{P_r}{\rho_r} + \frac{1}{2} \cdot (u_r - u_{SWr})^2 = e_b + \frac{P_b}{\rho_b} + \frac{1}{2} \cdot (u_b - u_{SWr})^2. \tag{20}$$

3.2 The Initial Values of the Flow in the Tube

At time t=0, the projectile enters the tube with supersonic velocity (u_P = 840 m/s). The velocity, u_{SW}, of the resultant shock wave is obtained by employing an impulsive piston-motion equation [14]

$$\frac{u_P}{a_2} = \frac{2}{\gamma + 1} \cdot \left(M_{SW} - \frac{1}{M_{SW}} \right), \tag{21}$$

where $M_{SW} = \frac{u_{SW}}{a_2}$ and the subscript 2 denotes zone 2 (Figure 2).

The jump conditions across the shock wave (equations 15–17) yield the initial flow parameters in zone 1.

As stated before, the rupture disc is designed to rupture once the shock wave reflects from it. At this time, the flow conditions at the location occupied by the rupture disc are found using shock-tube equations [14].

$$P_{rup} = \frac{2\gamma_{2P} \cdot M_{rup}^2 - \gamma_{2P} + 1}{\gamma_{2P} + 1} \cdot P_{2P}, \tag{22}$$

$$P_r = P_{rup} \cdot \left\{ 1 - \frac{\gamma_r - 1}{\gamma_{2P} + 1} \cdot \frac{a_{2P}}{a_r} \cdot \left(M_{rup} - \frac{1}{M_{rup}} \right) \right\}^{\frac{-2\gamma_r}{\gamma_r - 1}}, \tag{23}$$

$$u_{rup} = \frac{2}{\gamma_{2P} + 1} \cdot a_{2P} \cdot \left(M_{rup} - \frac{1}{M_{rup}} \right), \tag{24}$$

$$\rho_{rup} = \rho_r \cdot \left(\frac{P_{rup}}{P_r} \right)^{\frac{1}{\gamma_r}}, \tag{25}$$

where the subscript r refers to the conditions at the reflected region of the incident shock wave (Figure 9), the subscript 2P refers to pressurized zone between the ruptured disc and the free piston, and the subscript rup refers to the conditions initiated at the rupture disc location. In equations 22–24, the unknowns are P_{rup}, u_{rup}, and M_{rup}.

$u_{SWrup} = M_{rup} \cdot a_{2P}$ is the speed of the shock wave generated by rupturing the disc. In reality, at the time of the rupturing, the projectile is very close to the rupture disc, and hence, the shock wave that reflects from the rupture disc, reflects shortly from the projectile and overtakes/overwhelms the rupture disc shock wave.

4. Simulation Results

4.1 Coding and Run Parameters

The numerical solution was coded in FORTRAN 77 using the Watcom [15] Compiler. The code is run via an executable file in Microsoft Windows (Windows NT 4.0, Windows 95, or greater) environment. The program input is done interactively, and output data is automatically stored in ASCII files on the computer hard disc. The program prompts for lengths of the SRS tube sections; the weights of the projectile, free piston, and water; the initial pressure in zone 3; the projectile velocity; the hold pressures of the rupture diaphragm and shear ring. Other input parameters include the number of grid points per computational zone, time constants, run options, and output frequency. Typically, the number of grid points per computational zone varies from 11 to 51 points where computational zones 1 and 2 are more finely resolved. These grid resolutions were found to be adequate—higher resolution did not produce materially different results. The time steps of the solution were determined from the Courant-Friedrichs-Lewy condition [16]. When the free piston or the shock waves exit the tube, this causes a step pressure drop at the exit plane, and it was necessary for numerical stability to represent the step pressure as a time-wise exponential function. Typically, the time constant for the exponential function was chosen to be from 3 to 7 time steps. Run options include various default parameters; and in addition the choices of ignoring the water column friction and/or ignoring the transition tube and the rupture disc. Another run option is a Regula Falsi [17]-based iteration of either the initial pressure in zone 3, or the total mass of the distributed water, for a desired projectile exit velocity. For the simulation runs described here, the free-piston weight is fixed at 5 kg that is a practical weight for a polyethylene-made piston. Also, the projectile weight and muzzle velocity are fixed at the operational values of 46 kg and 840 m/s. The

pressure rating of the rupture diaphragm is chosen to be 750 psi (5.17 MPa) and the shear ring holds up to 500-psi (3.45 MPa) loading on the free piston. The transition tube length is fixed at 4.5 m.

4.2 Typical Flow Dynamics With and Without Inclusion of the Rupture Disc Process (Figure 10)

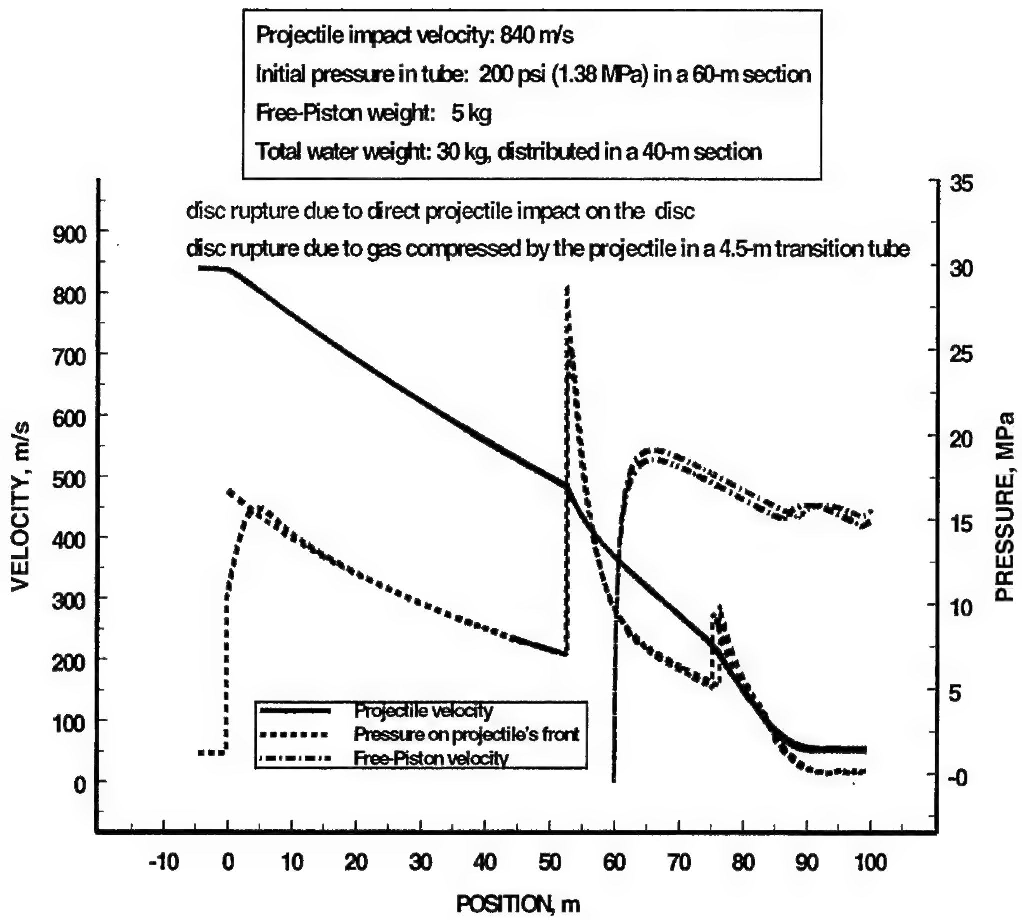

Figure 10. Dynamics in the SRS—effects of the transition tube/rupture diaphragm process.

Figure 10 demonstrates the flow dynamics in an SRS where the transition tube is 4.5 m long (shown at a negative position), the pressurized section (starts at the 0-m position) is 60 m long, and the guide section is 40 m long. Thus, the free piston is initially at the 60-m position. The pressure spikes on the projectile front are due to the reflection of the traveling shock wave that borders between the computational zones 1 and 2. In order for the projectile to experience deceleration lower than the allowed 1,600 g, the frontal pressure on the projectile

should not exceed 38 MPa. The free piston is accelerated rapidly to supersonic velocity, but the velocity eventually decreases because of the momentum transfer to the water swept by the free piston. As evident from Figure 10, if the transition tube/rupture disc process is not considered and the projectile is assumed to impact directly on the pressurized gas, the eventual effect on the projectile velocity is very small but the projectile would experience significant higher frontal pressure peak. In all following simulations the rupture disc process is taken into account.

4.3 Effects of the Water Friction (Figure 11)

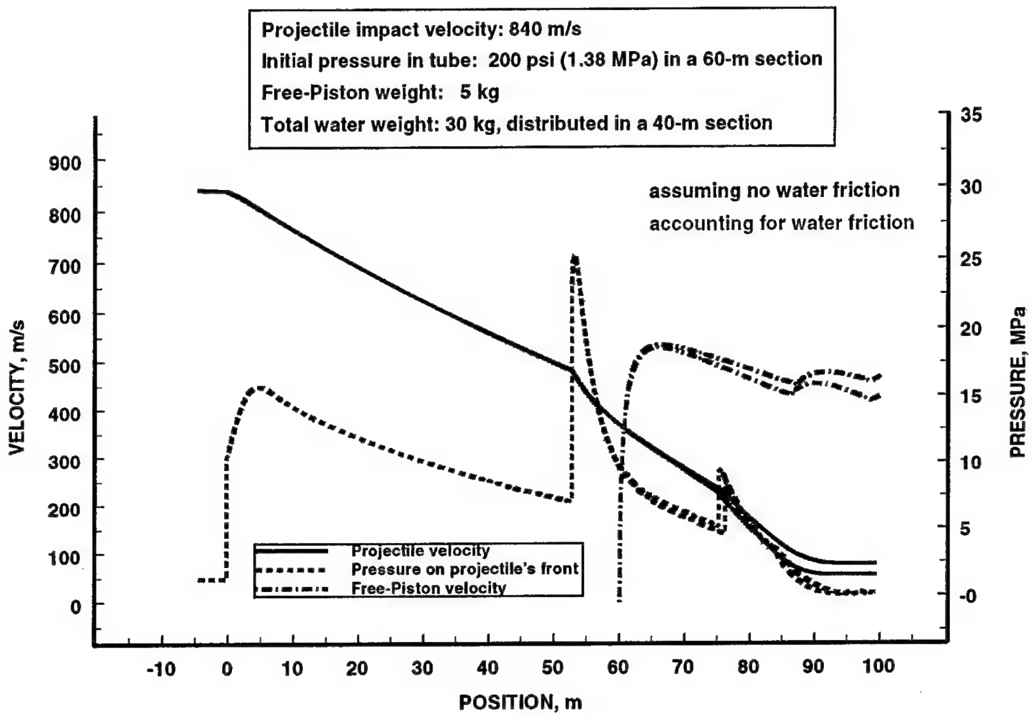

Figure 11. Dynamics in the SRS—effects of the water column friction.

Figure 11 demonstrates the effect of the water friction on the projectile velocity. If water friction is taken into account, the simulation indicates that the projectile will exit the tube with velocity that is about 20 m/s smaller than if water friction is neglected.

4.4 Flow Dynamics for Various Length and Pressure Parameters

In each of the following simulations, depicted in Figures 12–15, certain tube lengths are selected, as well as two initial tube pressures (200 psi and 300 psi), and the water mass necessary for a projectile exit velocity of 10 m/s is found using the Regula Falsi [17] iterative technique. In Figure 12's caption, the notation 100-60 stands for the total length (100 m) of the pressurized section and

the guide section of which the pressurized section (charged to either 200 or 300 psi) is 60 m. This is the same for the notations 70-50, 80-50, 80-60, in the captions of Figures 13, 14, and 15, respectively. The purpose of these simulations is to find optimal tube lengths and pressures. It is desirable to have short tubes that are lightly pressurized. However, it is not desirable to have multiple high-magnitude pressure spikes on the front of the projectile. Thus, a compromise has to be found with respect to tube size and initial pressures and the pressure loading on the projectile. Table 1 summarizes some of the results. It is apparent from Figures 12–15 and Table 1 that the 80-60 tube charged to 300 psi is a good choice. In this case, the maximum deceleration on the projectile is less than 1,000 g. Figure 16 depicts snap shots of the pressure and velocity distributions in the (four) computation zones of the 80-60/300-psi tube.

For this tube, the projectile will attain a relatively constant velocity of 10 m/s approximately 12 m before the exit. These values of distance and velocity are conservative in the sense that they allow for operational tolerances obviating a disastrous rebound of the projectile into the tube. Note that the maximum pressure loading on the free piston is much higher than on the projectile, but this is of little concern as the free piston is solidly built and it is expendable.

5. Summary and Conclusions

A novel soft recovery system based on ballistic compression concept and incorporating a free piston and water is physically sound. Such a system can recover controllably, within less than 120 m, a 155-mm (46 kg) projectile fired at 840 m/s. Because of the assumptions involved in the formulation, the numerical simulations are conservative with respect to deceleration limits and projectile travel requirement, and thus actual performance is expected to be better. The simulations indicate that the projectile can be stopped using a pressurized tube length of 60 m, and a guide section of 40 m. When using a 5-kg free piston, and 26.84 kg of water distributed in the guide section, the 60-m tube has to be pressurized initially to 300 psi (2.07 MPa). In this case, the maximum deceleration on the projectile is less than 1,000 g.

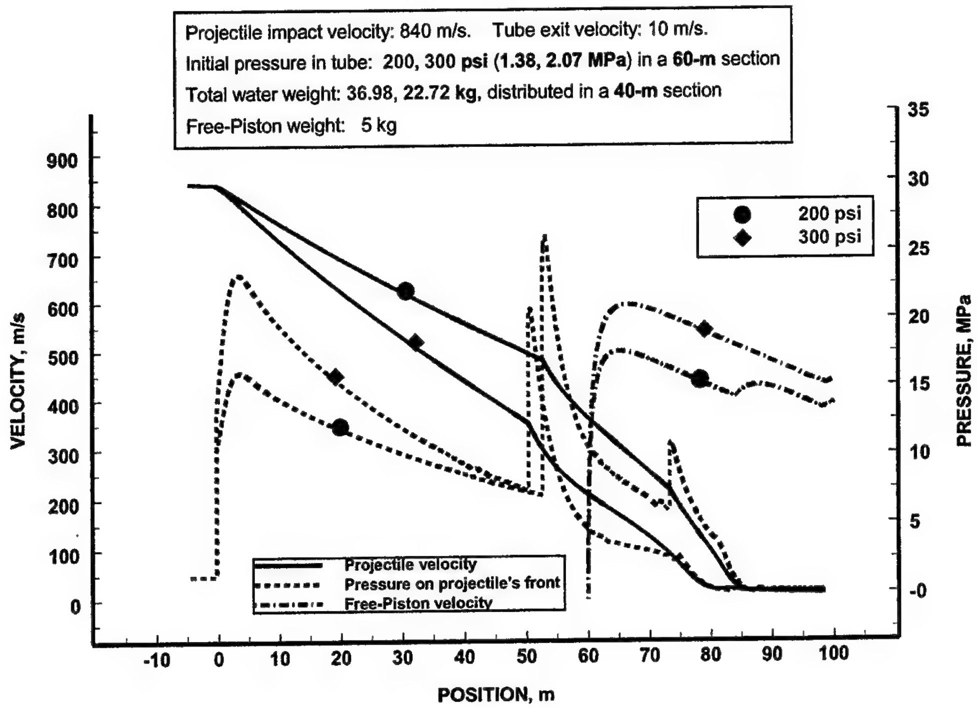

Figure 12. Dynamics for 100-60 SRS tube charged initially to 200 and 300 psi.

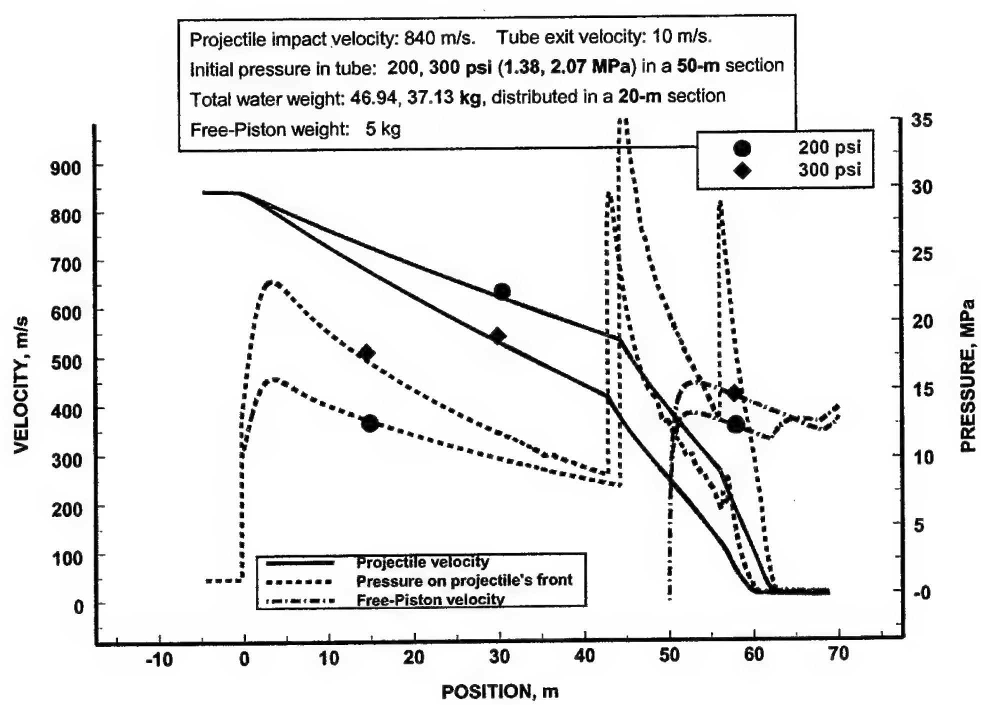

Figure 13. Dynamics for 70-50 SRS tube charged initially to 200 and 300 psi.

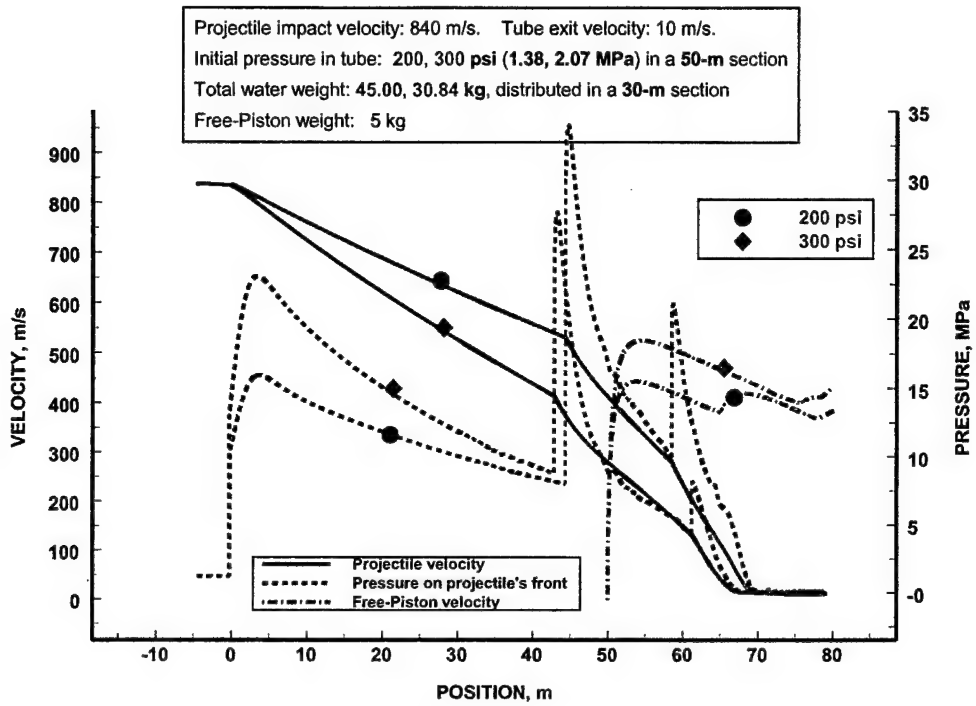

Figure 14. Dynamics for 80-50 SRS tube charged initially to 200 and 300 psi.

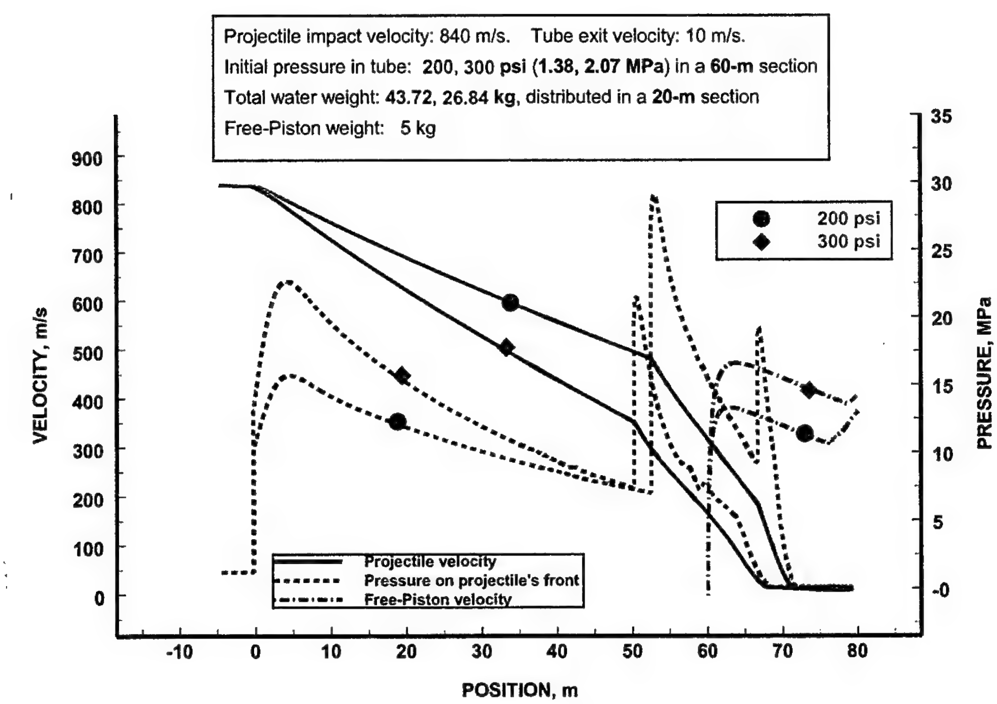

Figure 15. Dynamics for 80-60 SRS tube charged initially to 200 and 300 psi.

Table 1. Selected 155-mm SRS parameters.

Tube Total[a] Length (m)/ Pressurized-Section Length (m)/ Pressurization (psi)	Peak Pressure on the Projectile MPa (psi)	Peak Pressure on the Free Piston MPa (psi)	Water Mass[b] to Slow the 46-kg Projectile From 840 m/s to 10 m/s (kg)
100/60/300	23.16 (3,358)	70.61 (10,238)	22.72
100/60/200	25.93 (3,760)	56.09 (8,133)	36.98
80/60/300	22.62 (3,800)	70.85 (10,273)	26.84
80/60/200	29.00 (4,205)	56.23 (8,153)	43.72
80/50/300	27.75 (4,024)	76.96 (11,159)	30.84
80/50/200	34.03 (4,935)	59.89 (8,684)	45.00
70/50/300	29.52 (4,280)	76.96 (11,159)	37.13
70/50/200	36.74 (5,327)	59.87 (8,681)	46.94

[a] From the diaphragm to exit (the transition length from the vent holes to the diaphragm) is 4.5 m.

[b] The free-piston mass is 5 kg.

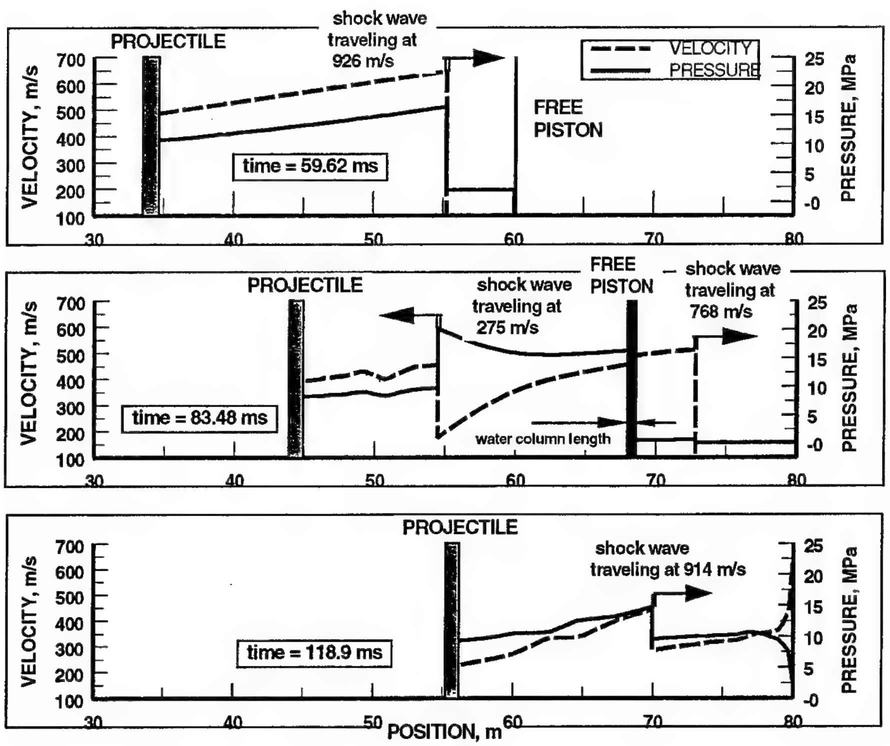

Figure 16. Snap shots of pressure and velocity distribution in the 80-60/300-psi tube.

6. References

1. Frydman, A. Personal communication with A. Birk. U.S. Army Research Laboratory, Aberdeen Proving Ground, MD, January 2000.
2. Carlucci, D. Personal communication with A. Birk. U.S. Army Research, Development, and Engineering Center, Dover, NJ, February 2000.
3. Wright, L. D. "An Investigation of High 'g' Launch, Soft-Recovery Test Facilities." Tank Systems Laboratory Technical Report No. RE-TR-71-12, U.S. Army Weapons Command, R&D Directorate, Rock Island, IL, March 1973.
4. Baer, P. G. "Digital Computer Analysis of a 155MM Soft Recovery System." Report No. 1634, U.S. Army Ballistic Research Laboratory, Aberdeen Proving Ground, MD, February 1973.
5. Clarke, E. V., C. R. Ruth, J. W. Evans, J. E. Bowen, J. R. Hewitt, and J. L. Stabile. "Large Caliber Projectile Soft Recovery." ABRL-MR-03083, U.S. Army Ballistic Research Laboratory, Aberdeen Proving Ground, MD, February 1981.
6. Evans, J. W., C. R. Ruth, and E. V. Clarke. "Soft Recovery Tests of a 155-MM Cannon Launched Guided Projectile Warhead, Type T." ARBRL-MR-03107, U.S. Army Ballistic Research Laboratory, Aberdeen Proving Ground, MD, May 1981.
7. Teng, R. N. "Ballistic Compression Decelerator." U.S. Patent No. 3,678,745, issued to McDonnell Douglas Corporation, July 1972.
8. Covey, W. B., J. R. Mastandrea, and R. N. Teng. "Projectile Recovery System With Quick Opening Valves." U.S. Patent No. 3,940,981, issued to McDonnell Douglas Corporation, March 1976.
9. Curchack, H. D. "Rifled Soft Recovery System." U.S. Patent 4,002,064, issued to U.S. Department of the Army, February, 1976.
10. Curchack, H. D., and A. D. Hahn. "Multi-Caliber Projectile Soft Recovery System." U.S. Patent No. 4,345,460, issued to U.S. Department of the Army, June 1980.
11. Kooker, D. E. "Modeling of Compaction Wave Behavior in Confined Granular Energetic Material." BRL-TR-3138, U.S. Army Ballistic Research Laboratory, Aberdeen Proving Ground, MD, August 1990.
12. IMSL. "User Manual/Math Library." Ver 1.1, Houston, Texas, 1989.
13. Bird, R. B., W. E. Stewart, and E. N. Lightfoot. *Transport Phenomena.* John Wiley & Sons, Inc., p. 204, 1960.

14. Thompson, P.A. *Compressible-Fluid Dynamic.* McGraw-Hill Book Company, Chapter 8, 1972.

15. Sybase Inc. Watcom FORTRAN77, Version 11.0, 1996.

16. Peyret, R., and T. D. Taylor. *Computational Methods for Fluid Flow.* Springer-Verlag, 1985.

17. Carnahan, B., H. A. Luther, and J.O. Wilkes. *Applied Numerical Methods.* John Wiley & Sons, Inc., Chapter 3.8, 1969.

NO. OF COPIES	ORGANIZATION
2	DEFENSE TECHNICAL INFORMATION CENTER DTIC DDA 8725 JOHN J KINGMAN RD STE 0944 FT BELVOIR VA 22060-6218
1	HQDA DAMO FDT 400 ARMY PENTAGON WASHINGTON DC 20310-0460
1	OSD OUSD(A&T)/ODDDR&E(R) R J TREW THE PENTAGON WASHINGTON DC 20301-7100
1	DPTY CG FOR RDA US ARMY MATERIEL CMD AMCRDA 5001 EISENHOWER AVE ALEXANDRIA VA 22333-0001
1	INST FOR ADVNCD TCHNLGY THE UNIV OF TEXAS AT AUSTIN PO BOX 202797 AUSTIN TX 78720-2797
1	DARPA B KASPAR 3701 N FAIRFAX DR ARLINGTON VA 22203-1714
1	US MILITARY ACADEMY MATH SCI CTR OF EXCELLENCE MADN MATH MAJ HUBER THAYER HALL WEST POINT NY 10996-1786

NO. OF COPIES	ORGANIZATION
1	DIRECTOR US ARMY RESEARCH LAB AMSRL D D R SMITH 2800 POWDER MILL RD ADELPHI MD 20783-1197
1	DIRECTOR US ARMY RESEARCH LAB AMSRL DD 2800 POWDER MILL RD ADELPHI MD 20783-1197
1	DIRECTOR US ARMY RESEARCH LAB AMSRL CI AI R (RECORDS MGMT) 2800 POWDER MILL RD ADELPHI MD 20783-1145
3	DIRECTOR US ARMY RESEARCH LAB AMSRL CI LL 2800 POWDER MILL RD ADELPHI MD 20783-1145
1	DIRECTOR US ARMY RESEARCH LAB AMSRL CI AP 2800 POWDER MILL RD ADELPHI MD 20783-1197

ABERDEEN PROVING GROUND

4	DIR USARL AMSRL CI LP (BLDG 305)

NO. OF COPIES	ORGANIZATION
2	SADARM PMO AMSTA AR FSP G D CARLUCCI PICATINNY ARSENAL NJ 07806-5000
2	NAVAL SURFACE WARFARE CENTER DAHLGREN DIV T E DORAN 17820 DAHLGREN RD DAHLGREN VA 22448-5100
	ABERDEEN PROVING GROUND
40	DIR USARL AMSRL WM BD R A BEYER A BIRK (5 CPS) A L BRANT L M CHANG T P COFFEE J COLBURN P J CONROY R A FIFER B E FORCH B E HOMAN S L HOWARD A J KOTLAR C LEVERITT M MCQUAID M S MILLER T C MINOR M J NUSCA J A VANDERHOFF A W WILLIAMS AMSRL WM BC P PLOSTINS V OSKAY J DESPIRITO J SAHU M BUNDY AMSRL WM MB A FRYDMAN (5 CPS) A ABRAHAM AMSRL WM TC R COATES AMSRL WM TB D KOOKER (5 CPS)

REPORT DOCUMENTATION PAGE

Form Approved
OMB No. 0704-0188

1. AGENCY USE ONLY *(Leave blank)*	2. REPORT DATE	3. REPORT TYPE AND DATES COVERED
	April 2001	Final, January–July 2000

4. TITLE AND SUBTITLE
A Novel Soft Recovery System for the 155-mm Projectile and Its Numerical Simulation

5. FUNDING NUMBERS
622618AH80

6. AUTHOR(S)
Avi Birk and Douglas E. Kooker

7. PERFORMING ORGANIZATION NAME(S) AND ADDRESS(ES)
U.S. Army Research Laboratory
ATTN: AMSRL-WM-BD
Aberdeen Proving Ground, MD 21005-5066

8. PERFORMING ORGANIZATION REPORT NUMBER
ARL-TR-2462

9. SPONSORING/MONITORING AGENCY NAMES(S) AND ADDRESS(ES)
PM SADARM, Picatinny Arsenal, NJ 07806-5000

10.SPONSORING/MONITORING AGENCY REPORT NUMBER

11. SUPPLEMENTARY NOTES

12a. DISTRIBUTION/AVAILABILITY STATEMENT
Approved for public release; distribution is unlimited.

12b. DISTRIBUTION CODE

13. ABSTRACT*(Maximum 200 words)*

There is a requirement to soft catch, without exceeding a deceleration rate of 1,600 g, and within less than 300 m, an unmodified 102-lb SADARM (Sense and Destroy Armor) projectile fired at 840 m/s. This report presents a soft-recovery concept and its numerical simulation. The concept entails aerodynamic deceleration of the projectile in a long tube attached to the gun barrel. The midsection of the tube is bound between a diaphragm and a free piston and is prepressurized to about 2 MPa. As the projectile enters the tube, the shock wave preceding it ruptures the diaphragm and the projectile decelerates as high pressure builds between it and the free piston. The piston disengages and travels forward scooping water. The waterlog that forms in front of the piston effectively increases the piston's mass and also induces braking force because of the water friction with the tube wall. The projectile's deceleration is controlled, and eventually the projectile exits the tube with a velocity of 10 m/s. The numerical simulation, based on the method of characteristics, incorporates unsteady one-dimensional fluid dynamics that captures the extensive wave dynamics. This report details the effects on the projectile's deceleration of the midsection length, initial pressure, and the water mass. From the simulation, it is possible to soft capture the SADARM projectile within 120 m.

14. SUBJECT TERMS
soft recovery, free piston, projectile, SADARM

15. NUMBER OF PAGES
33

16. PRICE CODE

17. SECURITY CLASSIFICATION OF REPORT	18. SECURITY CLASSIFICATION OF THIS PAGE	19. SECURITY CLASSIFICATION OF ABSTRACT	20. LIMITATION OF ABSTRACT
UNCLASSIFIED	UNCLASSIFIED	UNCLASSIFIED	UL

NSN 7540-01-280-5500

Standard Form 298 (Rev. 2-89)
Prescribed by ANSI Std. 239-18 298-102

INTENTIONALLY LEFT BLANK.

USER EVALUATION SHEET/CHANGE OF ADDRESS

This Laboratory undertakes a continuing effort to improve the quality of the reports it publishes. Your comments/answers to the items/questions below will aid us in our efforts.

1. ARL Report Number/Author ARL-TR-2462 (Birk) Date of Report April 2001

2. Date Report Received ____________________

3. Does this report satisfy a need? (Comment on purpose, related project, or other area of interest for which the report will be used.) ____________________

4. Specifically, how is the report being used? (Information source, design data, procedure, source of ideas, etc.) ____________________

5. Has the information in this report led to any quantitative savings as far as man-hours or dollars saved, operating costs avoided, or efficiencies achieved, etc? If so, please elaborate. ____________________

6. General Comments. What do you think should be changed to improve future reports? (Indicate changes to organization, technical content, format, etc.) ____________________

CURRENT ADDRESS

____
Organization

____
Name E-mail Name

____
Street or P.O. Box No.

____
City, State, Zip Code

7. If indicating a Change of Address or Address Correction, please provide the Current or Correct address above and the Old or Incorrect address below.

OLD ADDRESS

____
Organization

____
Name

____
Street or P.O. Box No.

____
City, State, Zip Code

(Remove this sheet, fold as indicated, tape closed, and mail.)

(DO NOT STAPLE)